


Electrochemical characterization of surfaces of galvanized steels under different exposure conditions using gel electrolytes

Andreas Heyn^{1,2}  | Moritz Meist¹ | Oliver Michael¹  |
Martin Babutzka^{3,4}  | Svenja Valet³  | Gino Ebell³ 

¹Institut für Werkstoff- und Fügetechnik, Otto-von-Guericke-Universität Magdeburg, Magdeburg, Germany

²Fakultät Ingenieurwissenschaften, Hochschule für Technik, Wirtschaft und Kultur, Leipzig, Germany

³Fachbereich 7.6 Korrosion und Korrosionsschutz, Bundesanstalt für Materialforschung und -prüfung (BAM), Berlin, Germany

⁴Berliner Hochschule für Technik (BHT), Berlin, Germany

Correspondence

Andreas Heyn, Otto-von-Guericke-Universität Magdeburg, 39106 Magdeburg, Germany.
Email: andreas.heyn@ovgu.de

Funding information

Deutsche Forschungsgemeinschaft, Grant/Award Number: 330472124; Bundesministerium für Wirtschaft und Energie, Grant/Award Number: 03TNH014A

Abstract

The corrosion behavior of galvanized steels and zinc components under atmospheric exposure depends mostly on the corrosion product-based cover layer formation under the prevailing conditions. The use of agar-based gel electrolytes makes it possible to use electrochemical methods to obtain a characteristic value from these cover layers that describe their current and future protective capacity. It is shown here that different states of galvanized steel can be distinguished very well under laboratory conditions and that this method is also suitable for use under practical conditions. Based on the characteristic values and assuming future time of wetness, it is very easy to draw up a forecast for the future corrosion rate, which provides plausible values.

KEYWORDS

atmospheric exposure, corrosion prediction, corrosion rate, electrochemical measurement, gel-electrolyte, protective layer, zinc coating

1 | INTRODUCTION

Components made of galvanized steel are an important part of today's infrastructure. They are extensively used in construction and are exposed to various atmospheric conditions. Galvanization, as a metallic coating, protects the steel from corrosion by decoupling the steel surface from atmospheric exposure. The durability of the steel structure will be ensured for a longer time because the corrosion rate of zinc can be up to 100 times lower than

that of structural steel, depending on the corrosivity of the atmosphere. The reduced corrosion rate is attributed to a protective layer of corrosion products that forms on the surface under atmospheric conditions. The composition and protective effect of this layer are significantly influenced by the exposure conditions and the type of zinc coating. The exposure conditions are defined by the duration and cycles of moisture film at the metallic surface (time of wetness [TOW]) and atmospheric contaminants containing corrosive components. Those

This is an open access article under the terms of the [Creative Commons Attribution-NonCommercial-NoDerivs](https://creativecommons.org/licenses/by-nc-nd/4.0/) License, which permits use and distribution in any medium, provided the original work is properly cited, the use is non-commercial and no modifications or adaptations are made.

© 2024 The Authors. *Materials and Corrosion* published by Wiley-VCH GmbH.

are primarily salts and SO_2 as well as various particles (dust, soot) from the air that adhere to the surface and significantly affect the time of wetness by retaining moisture on the surface. The classification of atmospheric corrosivity follows ISO 9223,^[1] where corrosivity categories are derived from the mass losses in the first year of outdoor exposure of standard samples according to ISO 9226.^[2] Reference values for corrosion progress can be found in ISO 9224,^[3] which provides values for zinc, steel, aluminum, and copper. These values are based on the outdoor exposure of standard samples at characteristic locations for 1 year, as regulated in ISO 8565.^[4] In theory, according to these normative regulations, the design of zinc coating thicknesses for steel construction components could be possible, aligning with the expected corrosivity and the desired service life of the components, but this is rarely implemented in practice.

Corrosion rates determined by standard samples should only be considered as orientation values and do not allow for direct transferability to a real structure made of galvanized steel under specific exposure conditions. Deviating from generally assumed exposures, construction- or location-specific microclimates, such as persistently moist surfaces, or special climates with locally increased pollutant concentrations (e.g., due to de-icing salts and sulfates), can lead to significantly different corrosion rates on the same structure. Therefore, determining the actual and possibly also estimating the future corrosion rate of galvanized steel on real structures is an important issue for which there has been no satisfactory solution so far. A nondestructive measurement of the remaining coating thickness with commercially available devices only shows reasonably reliable loss of metal and thickness after many years, as the corrosion rates are generally very low. In addition, this only determines the metal loss from the past and does not allow for an estimation of future corrosion rate. To estimate future corrosion rates, information about the protective properties of the layer of corrosion products present on the structure is important as soon as it is in equilibrium with the environment. Thus, a relatively stationary state exists. The point in time when a stationary state is reached also depends on the specific material and exposure factors. There are indications that the layer formation can be completed after only a few months to a year, and thereafter the corrosion rate significantly decreases.^[5]

The corrosion rate of galvanized steel is significantly influenced by the formation of protective layers on the surface, which can affect both anodic and cathodic processes depending on their characteristics. The extent to which protective layers on zinc can perform largely hinges on their composition, which, in turn, dictates their stability under various environmental conditions.^[6–8] Protective layers typically originate from corrosion reactions

involving the material and the constituents of the surrounding electrolyte. Persson et al. provide a comprehensive summary of the current knowledge regarding the composition of protective layers on zinc, considering varying global exposure conditions.^[9] Odneval et al. also highlight the impact of runoff on both the composition and the corrosion protection of protective layers on galvanized steel,^[10] including the chronological sequence of their formation. Extensive literature indicates that the compound hydrozincite, $\text{Zn}_5(\text{CO}_3)_2(\text{OH})_6$, is among the most stable of such layers, in contrast to corrosion products containing sulfates or chlorides, or simpler compounds like zinc oxide or zinc hydroxide, which show lesser durability. Generally, the surface compositions are diverse, with noticeable variations even within the same structure. This variability is influenced by factors, such as the orientation of the components (horizontal, vertical, or directional), their positioning (exposed to rain or protected), and the mass of the component, which can alter the drying of the surfaces. For instance, Ji et al.^[11] demonstrate how the orientation of an externally stored galvanized wire sample affects the composition of its protective layers.

It can be inferred that the respective protective layer on a galvanized component, after a certain period of exposure, reaches a kind of equilibrium with environmental influences, which, in turn, determines the stability, protective capacity, and future corrosion rate. Therefore, if one can directly determine the protective capacity of the protective layer on-site on an exposed component, a much more practically relevant result is obtained. However, several challenges to this approach need to be addressed. First, handling liquid electrolytes for electrochemical measurements is not easy, especially when it comes to different measuring positions (vertical or overhead) or uneven surfaces. Furthermore, it must be considered that the composition of the liquid test electrolyte also influences the measurement results, as electrochemical and chemical reactions occur between the metal, protective layer, and test electrolyte during the measurement. Considering the equilibrium-dependent stability of the protective layer, as described by Folton and Swinehart,^[12] exposure to aqueous electrolytes cannot provide information about the current prevailing stability of the protective layer, as the equilibrium is disturbed within a few tenths of a second.

The use of agar-based gel electrolytes simplifies the measurements, as the aqueous test electrolyte is retained in the gel. A thin electrolyte film of a few micrometers forms between the gel and the surface to be tested,^[13,14] which makes the electrochemical measurements possible. The special properties of agar-based gel electrolytes have also been exploited by Cano et al. who used gels for

measurements on historical sculptures.^[15] Monrrabal has published work on the use of agar gels for the investigation of stainless steels^[16] as well as structural steel and galvanized steel.^[17] The use of agar gels for electrochemical investigations on galvanized steels was also previously presented by Vanbrabant et al.^[18]

To measure as minimally invasively as possible on metal surfaces with naturally formed corrosion product layers, the test electrolyte in the gel can be selected so that it corresponds as far as possible to the natural exposure of the surface, for example, condensate or rainwater. Water-soluble substances bound in the corrosion product layers are transferred into the thin electrolyte film of the gel after the gel has been applied and form a natural electrolyte film, as is also the case when the surface is moistened in practice, for example. This type of measurement is comparable to natural moistening in practice and can therefore be considered minimally invasive for the examination, that is, it only slightly changes the surface to be examined throughout the measurement of a few minutes, depending on the corrosion product layer formed, for example, hydrozincite. If easily soluble coating components such as zinc hydroxide and zinc oxide are present, these are reduced because of the equilibrium disturbance and results are inevitably obtained that correctly predict lower coating stabilities. This can be used to prove the influence of layers of corrosion products on the corrosion behavior of zinc, as Babutzka and Heyn were able to show.^[19–21] Minimally invasive electrochemical investigations with agar gels without any additives to study corrosion product layers on zinc were then also carried out by Langklotz et al.^[22] and Valet et al.^[23] They showed the correlation with special corrosion product species^[22] and the derivation of the surface layer resistance^[23] from linear polarization resistance (LPR) measurements.

This publication shows that the protective effect of different surface layers on galvanized steel can be differentiated with simple electrochemical measurements (LPR) using gel electrolytes under laboratory as well as practical conditions. By exposing galvanized steel samples to a natural atmosphere and targeted corrosive exposure, different surface layer conditions were generated and characterized using electrochemical and surface analytical methods. In addition, electrochemical measurements were carried out using mobile measurement technology on structures in Germany that have been in use for years. It was shown that valuable information on the condition of the structures can be obtained, including information on microclimates that can lead to different corrosion rates on the same component in the future. Using an expected average duration of time of wetness and the measured electrochemical parameters, an estimate of the future corrosion rate can be made. Its significance is discussed in this article.

2 | EXPERIMENTAL

2.1 | Materials

The sample material used for the electrochemical and analytical studies consisted of continuous hot-dip galvanized steel sheets with a coating thickness of 20 μm , which will be referred to as “HDG” in the following. The test sheets were obtained as Test Panels Gardobond® (Chemetall GmbH) and labeled as HDG7 (typical for the automotive industry). The surfaces of the samples were degreased by the manufacturer and did not have any other surface treatments or conversion layers. For comparison purposes, some samples were pickled (5 min in 1 M NaOH at 22°C).

2.2 | Exposure of sample material

Several HDG samples were exposed at a test site in Magdeburg (urban atmosphere, C2 category) for up to 75 weeks. The test stand is located 3 m above the ground and is approximately 4 m away from any vegetation or buildings. The sample holder is inclined at 15° and faces west. The samples were mounted flat on the holder so that the top side was exposed to rain (open air), while the underside was not (sheltered/ventilated). The gap between the sample holder and the underside was about 5 cm. The exposure period spanned from April 2021 to October 2022. Daily temperatures, relative humidity, and rain events were obtained from the German Weather Service. Data from the Magdeburg weather station (ID 3126) are considered as transferable to the exposure site. For the exposure period, average values were determined for temperature (12.2°C), relative humidity (74%), and rainfall (480 mm/year). Based on this information and an earlier evaluation of weather data from 2010 to 2016 for the Magdeburg site,^[24] an average wetting duration of 38% was determined for further consideration. This value is based on periods during which the following conditions are met: temperature > 0°C, relative humidity > 80%, and rainfall events > 5 mm/day. Data on SO₂ and chloride levels were not collected in the vicinity of the site and therefore not documented. However, it can be assumed that the values are within a noncorrosion relevant range. Information on the exposure conditions of additional practical investigation objects can be found in the following section.

One sample of the HDG material was subjected to a 7-day neutral salt spray (NSS) test according to DIN EN ISO 9227^[25] to induce a highly corroded reference state and then characterized electrochemically. The samples were dried after the test and the salt deposits were removed with a plastic brush. Firmly adherent corrosion products remained on the sample surface.

2.3 | Investigated structures

This section describes three different structures that incorporated galvanized steel and had been exposed to typical local atmospheric conditions for several years to decades. On these structures, the electrochemical determination of protective layer resistances using agar-based gel electrolytes, as described in this article, was carried out at various locations. Additionally, the surfaces were partially examined for contamination with corrosive ions using wipe samples and corresponding analytical methods.

2.3.1 | Measurement object 1: “Lenne Bridge”

The “Lenne Bridge” measurement object is an HDG steel bridge that was 33 years old at the time of measurement in 2020. It is located on the German federal highway B236 in the area of the city of Werdohl and crosses the Lenne river. The average annual temperature here is 9.8°C, with a cumulative annual rainfall of 1008 mm recorded. Figure 1 shows a photo of the bridge. The GPS data set for this location is: 51°15′50.5″ N and 7°44′35.5″ E.

At this site, LPR measurements were conducted for 18 min, along with polarization curves and electrochemical impedance, at various spots one to three times. The horizontal measurement points were the top and bottom sides of HDG steel beams, which do not exhibit an undisturbed η layer (approximately 99% Zn) due to the presence of iron–zinc alloy phases from the ζ layer extending to the surface. A vertical measurement point involved an HDG post, which was measured both in its



FIGURE 1 Measurement object “Lenne Bridge” made of galvanized steel over the Lenne river on the German federal highway B236. [Color figure can be viewed at [wileyonlinelibrary.com](https://onlinelibrary.wiley.com/terms-and-conditions)]

current state and after the mechanical removal of the protective layer by grinding.

2.3.2 | Measurement object 2: “Waldkappel Motorway Bridge”

The second measurement object is the Waldkappel/Bischhausen motorway bridge on the A44 motorway. Measurements were conducted on an HDG bridge girder. Due to the structural design of the bridge, the HDG girders are not classified as being freely rained upon. At the time of measurement in 2021, the motorway was not yet operational, but the bridge had already been completed for 5 years. The average annual temperature for Eschwege in 2021, located near the site, was 9.3°C, the cumulative annual rainfall was 572 mm, and the average annual relative humidity was 79%.

At this measurement object, swipe samples were taken from the inner and outer surfaces of the girders to determine the deposited levels of corrosion-relevant pollutants, as shown in Figure 2. Up to five individual LPR measurements were conducted at these points after a 10-min waiting period and one electrochemical impedance measurement per location. The GPS data set for this location is 51°08′36.6″ N and 9°56′11.6″ E.

2.3.3 | Measurement object 3: “Motorway Guardrails in Bergisch Gladbach”

The third measurement object is a galvanized motorway guardrail on a test track of the federal motorway “BAB” A4 near Bergisch Gladbach, maintained by the Federal Highway Research Institute (BASt). Two different guardrail beams were measured in 2019 after 17 years of service. Swipe samples were taken from both rails. One guardrail beam was piece-galvanized (Zn) and the other was continuous HDG (ZnAl). The GPS data set for this location is 50°57′00.8″ N and 7°08′43.7″ E. Figure 3 shows the measuring points on the two types of guardrails.

Due to the surfaces being extremely contaminated, they were first cleaned with water and surfactants before electrochemical testing to ensure proper contact of the gel with the surface of the galvanized steel. LPR measurements were performed on both the piece-galvanized (Zn) and continuous HDG (ZnAl) guardrail beams. The average annual temperature near the measurement site is 10.6°C, with a mean annual rainfall of 1125 mm, plus undefined amounts of spray water and mist. The average annual relative humidity

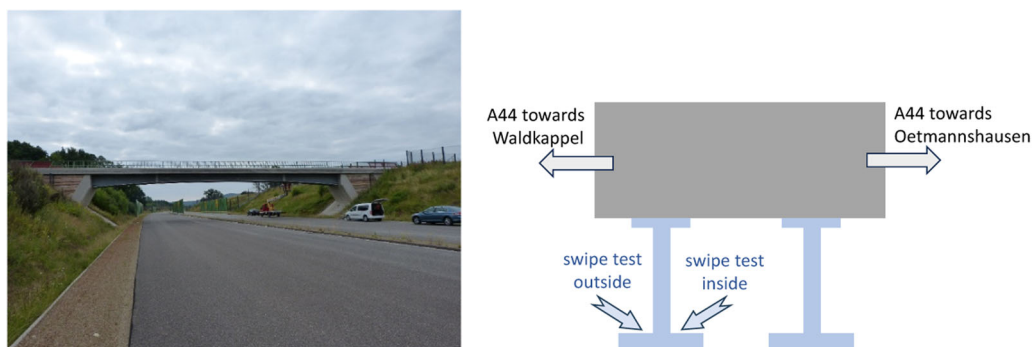


FIGURE 2 Measurement object “Waldkappel Motorway Bridge” near Waldkappel/Bischhausen, including a schematic drawing of the swab sampling locations on the outer and inner surfaces of a girder. [Color figure can be viewed at [wileyonlinelibrary.com](https://onlinelibrary.wiley.com/doi/10.1002/maco.202414389)]



FIGURE 3 Measurement object 3 near Bergisch Gladbach: piece-galvanized guardrail on the left, continuous hot-dip galvanized guardrail on the right. [Color figure can be viewed at [wileyonlinelibrary.com](https://onlinelibrary.wiley.com/doi/10.1002/maco.202414389)]

was 77%. To better assess the measurements, additional tests were conducted on pure zinc after 0–3 years of open-air weathering in Berlin and on ZnAl in its initial state.

2.4 | Gel electrolytes

The gel electrolytes were prepared using agar powder from Merck. To do this, 3 wt% of the powder was mixed with 97 mL of neutral distilled water at room temperature and brought to a boil while stirring. The agar melts and dissolves in the water. After maintaining the solution at approximately 100°C for 10 min, it was cooled to 65°C while stirring and then poured into Plexiglas containers to form a gel plate with a thickness of 4 mm. This gel plate was then stored for at least 24 h at 5°C. Before being used as a measuring electrolyte, they were brought back to room temperature. For use as a measuring electrolyte, circular pads with a diameter of 11.3 mm were cut out using a hole punch, resulting in a contact area with the sample of 1 cm². The gels remain largely pH-neutral, with an average pH value of 6.4.

For field measurements, gels were prepared in the same manner, but with a thickness of about 3 mm and a

diameter of 19 mm, resulting in a measurement area of 2.85 cm².

2.5 | Measurement setup and electrochemical methods

For measurements on exposed samples and the original and pickled states, circular gel pads with an area of 1 cm² were placed on the sample surface, and the counter (metal mesh made of titanium with precious metal-activated oxide) and reference electrodes (saturated Ag/AgCl electrode, $E_0 = 197$ mV vs. SHE) were connected on top of the gels. Care was taken to ensure that the electrodes had sufficient contact with the gel without exerting too much pressure that could cause the electrolyte to escape from the sides of the gels or break them. Rheological studies of agar gels^[14] indicated that for a 3% gel, the applied pressure should not exceed 0.6 N/cm² (threshold value for flow stress). Electrochemical measurements were conducted immediately after making contact.

For the electrochemical measurements in the laboratory, a Gamry Instruments Reference 600+

potentiostat was used. Initially, the open circuit potential (OCP) was measured for 20 min. During this measurement, a LPR measurement was conducted every minute with a ± 10 mV polarization and a polarization rate of 1 mV/s. The LPR measurement was automatically evaluated by the measurement program in the ± 5 mV range, which is acceptable in terms of linearity. The OCP value before the LPR measurement and the LPR value were recorded. This was followed by a measurement of the electrochemical impedance at the last measured OCP value in a frequency range from 100 kHz to 0.1 Hz with a 10 mV amplitude and 10 rounds for each frequency. Then, a polarization measurement from -1.3 to -0.6 V versus $\text{Ag}/\text{AgCl}_{\text{sat}}$ was carried out at a rate of 2 mV/s to characterize the cathodic and anodic regions. Each sample condition was measured at least five times.

For the electrochemical measurements on the practical objects, a portable PalmSens 4 potentiostat from PalmSens was used. OCP, LPR, electrochemical impedance spectra, and polarization curves were recorded.

2.6 | Analytical methods

The states of the HDG samples in their original condition, HDG after 7 days in the NSS test, and the HDG samples exposed for 75 weeks with both top and bottom sides were examined using scanning electron microscopy/energy dispersive X-ray spectroscopy (SEM/EDS). A Zeiss EVO 15 instrument equipped with an integrated SmartEDX detector was employed for this purpose. Comparative images of characteristic areas of the samples were taken in the backscattered electron (BSE) mode, and specific areas were analyzed using EDS.

3 | RESULTS

3.1 | Measurements on exposed samples and samples from the NSS test

3.1.1 | Electrochemical measurements

The averaged trends of the OCP and LPR measurements from all the tests are depicted in Figure 4. In the initial minutes after applying the gel, the corrosion system approaches a steady state. It is presumed that the wetting with the electrolyte film of the gel electrolyte slightly alters or forms new corrosion products. In samples without a protective layer, the electrolyte reacts with the bare zinc surface, resulting in the formation of minimal new corrosion products. Hence, a certain amount of time is needed until the potentials no longer change significantly. After 10 min, the system can be considered to have reached a sufficient level of stability to determine an LPR value characteristic for each state. The mean values and standard deviations for OCP and LPR after 10 min of electrolyte contact are summarized in Table 1.

The HDG sample with the original surface and the pickled state have approximately the same potential levels, but they differ in the LPR value. Apparently, the zinc oxide layer formed in air and over an unknown period on the original state sample leads to a slightly higher LPR value of about $50 \text{ k}\Omega \text{ cm}^2$, compared to the pickled surface with about $30 \text{ k}\Omega \text{ cm}^2$. Due to the formation of a zinc oxide layer when the sample is removed from the pickling bath into the atmosphere, the pickling process could not produce zinc oxide-free surface conditions.^[26] A completely different picture emerges from the sample after a 7-day exposure to the salt spray test. The heavily corroded surface, with macroscopically visible white rust deposits and a

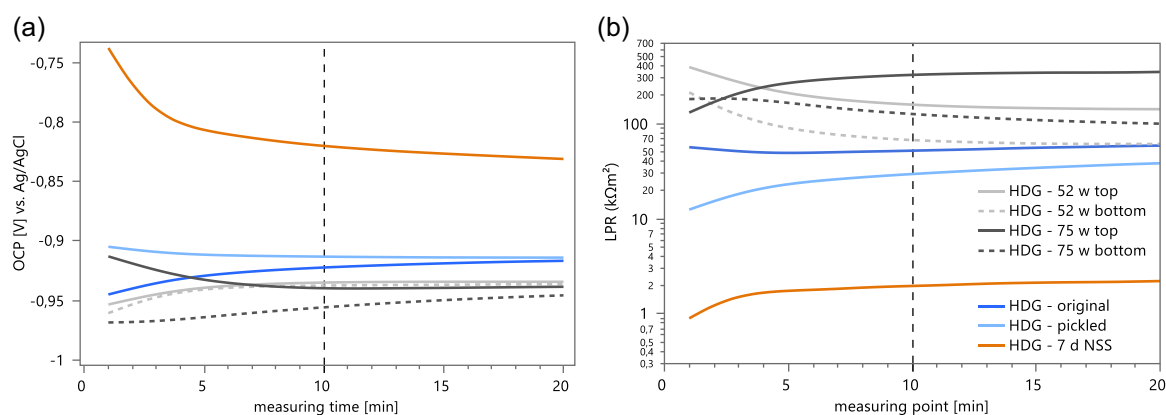
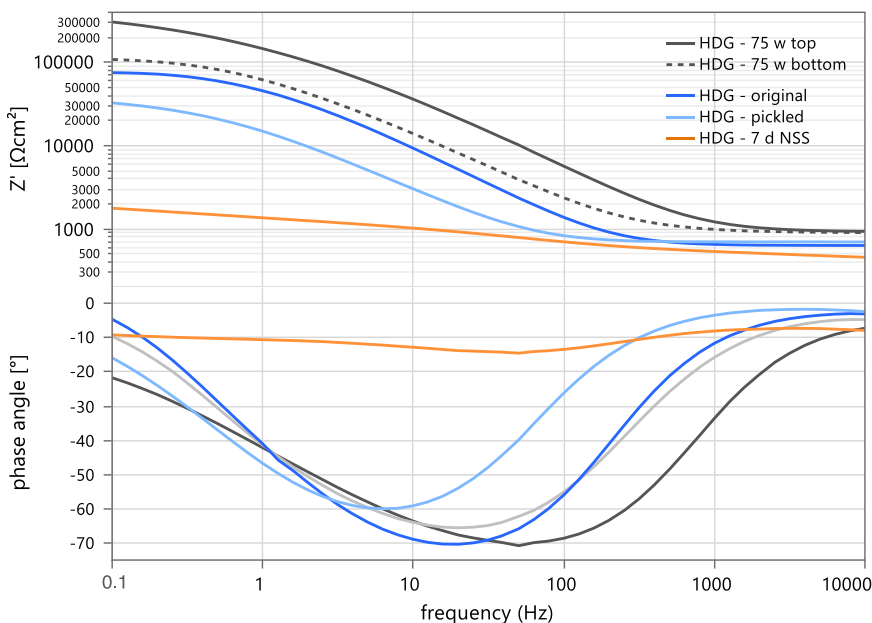


FIGURE 4 Averaged trends of OCP (a) and LPR values (b) over 20 min on HDG samples with various surface conditions. [Color figure can be viewed at wileyonlinelibrary.com]

TABLE 1 Mean values and standard deviations of OCP and LPR from measurements on HDG samples in different states, measured after 10 min of electrolyte contact.

| Material | Condition | N | OCP (mV), mean | OCP, SD | LPR ($\text{k}\Omega \text{cm}^2$), mean | LPR, SD |
|--------------|----------------------|---|----------------|---------|--|---------|
| HDG | Original | 5 | -922.3 | 17.7 | 52.1 | 7.4 |
| HDG | Pickled | 5 | -913.1 | 14.5 | 29.6 | 2.9 |
| HDG | 7-Day NSS | 8 | -819.9 | 164.1 | 2.1 | 0.9 |
| HDG 52 weeks | Exposure bottom side | 5 | -937.5 | 6.8 | 70.6 | 27.0 |
| HDG 52 weeks | Exposure top side | 5 | -934.9 | 2.2 | 159.3 | 19.5 |
| HDG 75 weeks | Exposure bottom side | 5 | -955.8 | 4.2 | 128.0 | 22.8 |
| HDG 75 weeks | Exposure top side | 5 | -939.8 | 12.1 | 329.4 | 42.4 |

FIGURE 5 Electrochemical resistance Z' and phase angles of the investigated sample states after 20 min of electrolyte contact. [Color figure can be viewed at wileyonlinelibrary.com]



roughened surface due to corrosion, shows the lowest LPR values at only about $2 \text{ k}\Omega \text{cm}^2$. Initially surprising are the OCP values, which are about 100 mV more positive compared to the original state and the pickled sample. Normally, more active samples also show more negative OCP values. However, this phenomenon can be explained based on the polarization curves. As expected, the samples after 52 or 75 weeks of open-air exposure show significantly higher LPR values and, again surprisingly at first, more negative OCP values. The differences between the top side of the weathered samples, which is exposed to rain, and the bottom side, which is sheltered from rain but still exposed to humidity and possible pollutants (ventilated), are interesting. The underside shows an LPR value that is only about half as high. The longer exposure time of 75 weeks compared to 52 weeks can also be seen in the LPR values, indicating a further

increase of about 80%–100% on both the top and bottom sides.

The electrochemical impedance spectroscopy (EIS) measurements conducted after the 20-min OCP/LPR measurements revealed similar dependencies as the LPR values, as shown in Figure 5. The impedances at the lowest frequency of 0.1 Hz show approximately the same gradation. Additionally, it is noticeable that the phase angles of the longer-exposed HDG samples broaden over the frequency range. The impedances at frequencies $>1000 \text{ Hz}$ provide an indication of the electrolyte resistance. When using similarly composed agar gels, a change can be attributed to the accumulation of ions from zinc or soluble corrosion products or dissolved accumulated pollutants in the electrolyte film between the gel and the sample surface. This explains why the sample after 7 days in the NSS test exhibits the lowest

electrolyte resistance, as the sample is most active and residual soluble salts remain on the surface, which were not completely removed. The samples with stable protective layers exhibit the highest electrolyte resistances, as these layers are less soluble, thus inhibiting the formation of zinc ions from corrosion processes and protecting the zinc from corrosion.

The polarization tests conducted following the EIS measurements provide insight into the cause of the reaction inhibition by the protective layers, as seen in Figure 6. In the samples after 7 days in the salt spray test, the current densities are the highest, that is, the least inhibited. The pickled sample and the one in its original state show significantly lower current densities and inhibition in both the anodic and cathodic regions. Particularly noticeable is the inhibition of the cathodic current densities in the weathered samples, which increases further with longer exposure. The significantly stronger inhibition of the cathodic partial reaction is responsible for the OCP values (compare Figure 4 and Table 1) being more negative in samples with protective layers, as the potential values in the equilibrium state shift more into the negative range.

3.1.2 | Analytical studies on exposed samples and samples from the salt spray test

The HDG samples in their original state, HDG after 7 days in the NSS, and the HDG samples exposed for 75 weeks, both top and bottom sides, each exhibited their typical visual macroscopic appearance. The original samples had a shiny silver appearance, while the samples exposed for 75 weeks turned a dull gray to varying

degrees due to corrosion reactions and the formation of protective layers. The top side of the exposed samples appears slightly darker compared to the bottom side. The HDG sample showed pronounced white and approximately 5% reddish corrosion products, originating from the steel sheet beneath the zinc coating after 7 days in the NSS. This indicates that the corrosion rate in the NSS over the 7 days of exposure must have been high enough to partially dissolve the 20 μm zinc coating through corrosion processes, leading to the corrosion of the underlying iron.

Comparative SEM images confirm the visual appearance. Figure 7 compares the four examined states in BSE mode at $\times 50$ magnification.

The comparative images in BSE mode at $\times 500$ magnification in Figure 8 reveal finer details in the respective sample states. The original state sample appears free from any corrosion products. In contrast, the NSS sample shows edges with apparently loose corrosion products at the boundary of slightly brighter areas, which, according to EDS analyses, are very rich in iron and thus correspond to the heavily dissolved areas where the steel beneath the zinc coating is already providing an EDS signal. In the exposed samples, especially in the areas of grain boundaries, enhanced dissolution or adhering corrosion products are visible. On the top side, these phenomena are more frequent, and the darker areas, identified as zinc corrosion products, are relatively evenly distributed across the surface. On the bottom side of the exposed sample, the distribution of corrosion products is not as uniform. This could be due to the lack of liquid water, which does not have direct access to the bottom side of the samples, preventing an even distribution of corrosion products.

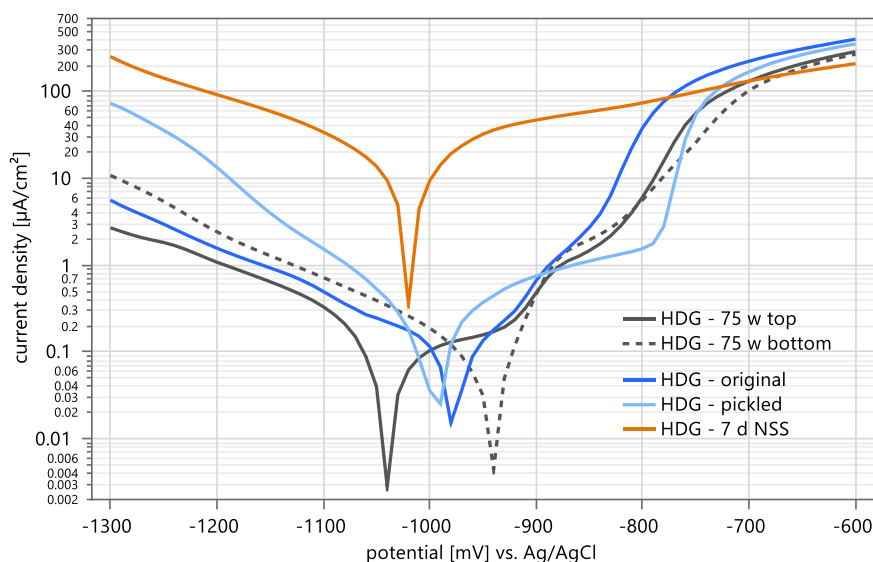


FIGURE 6 Polarization curves of the investigated sample states after approximately 40 min of electrolyte contact. [Color figure can be viewed at wileyonlinelibrary.com]

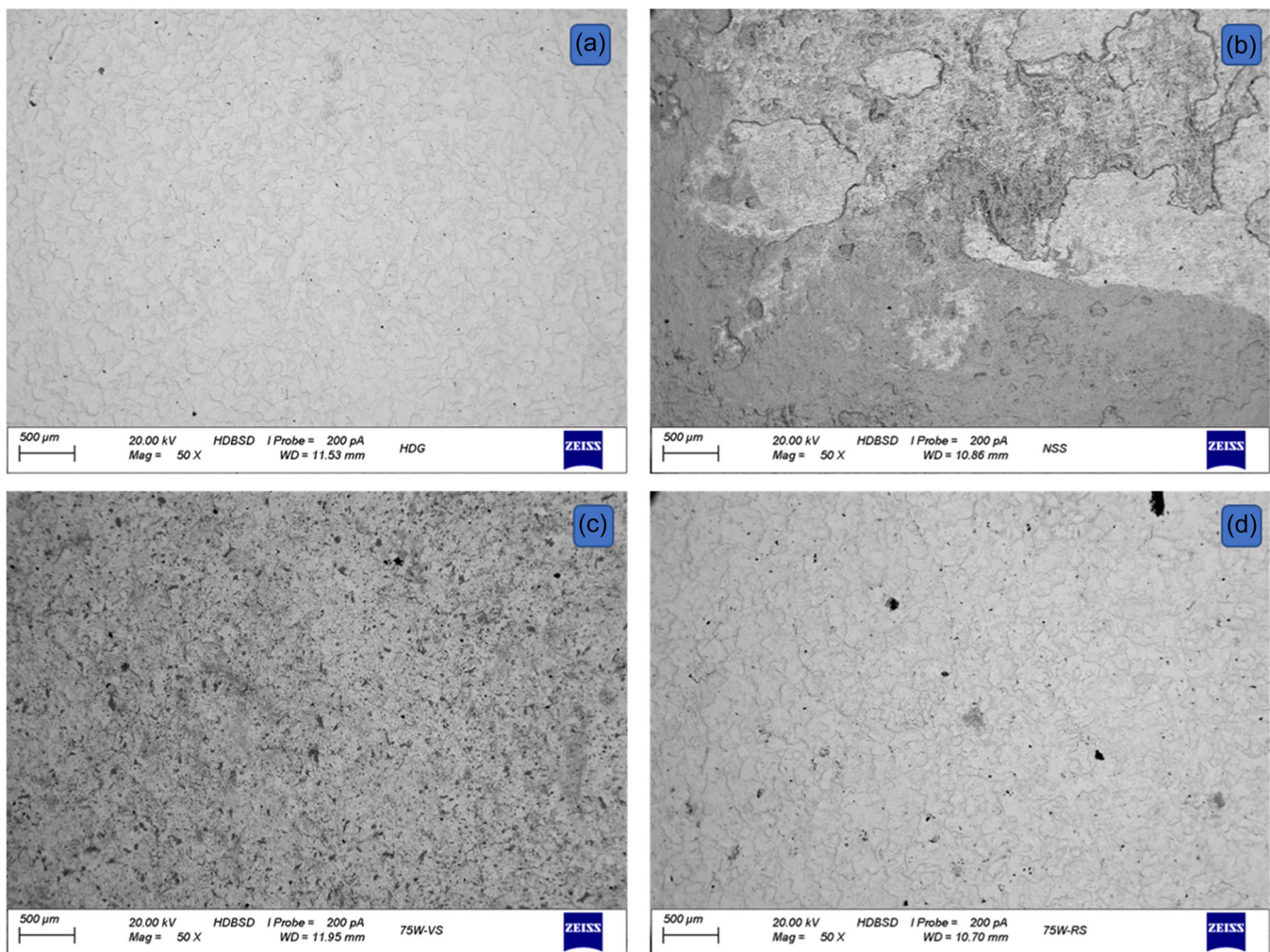


FIGURE 7 Comparative representation of the sample states: (a) HDG original, (b) HDG 7 days NSS, (c) HDG after 75 weeks exposure in C2 atmosphere top side, and (d) bottom side, at $\times 50$ magnification. [Color figure can be viewed at [wileyonlinelibrary.com](https://onlinelibrary.wiley.com/terms-and-conditions)]

3.2 | Measurements on practical objects

3.2.1 | Measurements on object 1: “Lenne Bridge”

In the measurements at the “Lenne Bridge” object, only individual measurements could be conducted for practical reasons. Both the top and bottom sides of the bridge beams were measured. All values are compiled in Table 2.

It was observed that the top side had a potential of about 100 mV more positive compared to the bottom side, while simultaneously having a lower protective layer resistance of only $47 \text{ k}\Omega \text{ cm}^2$ compared to $165 \text{ k}\Omega \text{ cm}^2$ on the bottom. This is likely due to the long service life and open exposure to precipitation, leading to partial removal of the galvanization down to the substrate. Consequently, the higher iron content relative to the measurement surface affects the potential formation

(shifting in the positive direction), and the locally actively corroding substrate components result in a lower integral protective layer resistance, which does not reflect the protective effect of a zinc protective layer. The vertically positioned post, however, has a significantly higher protective layer resistance of over $400 \text{ k}\Omega \text{ cm}^2$, and the potential here is more negative, both indicating a protective layer and no exposed substrate. After mechanically removing the protective layer by grinding (activation), the LPR value is $12 \text{ k}\Omega \text{ cm}^2$ low.

3.2.2 | Measurements on object 2: “Waldkappel Motorway Bridge”

At the “Waldkappel Motorway Bridge” object, measurements were conducted at several locations on a galvanized steel girder. The measurement points can be considered as external and internal surfaces, given their

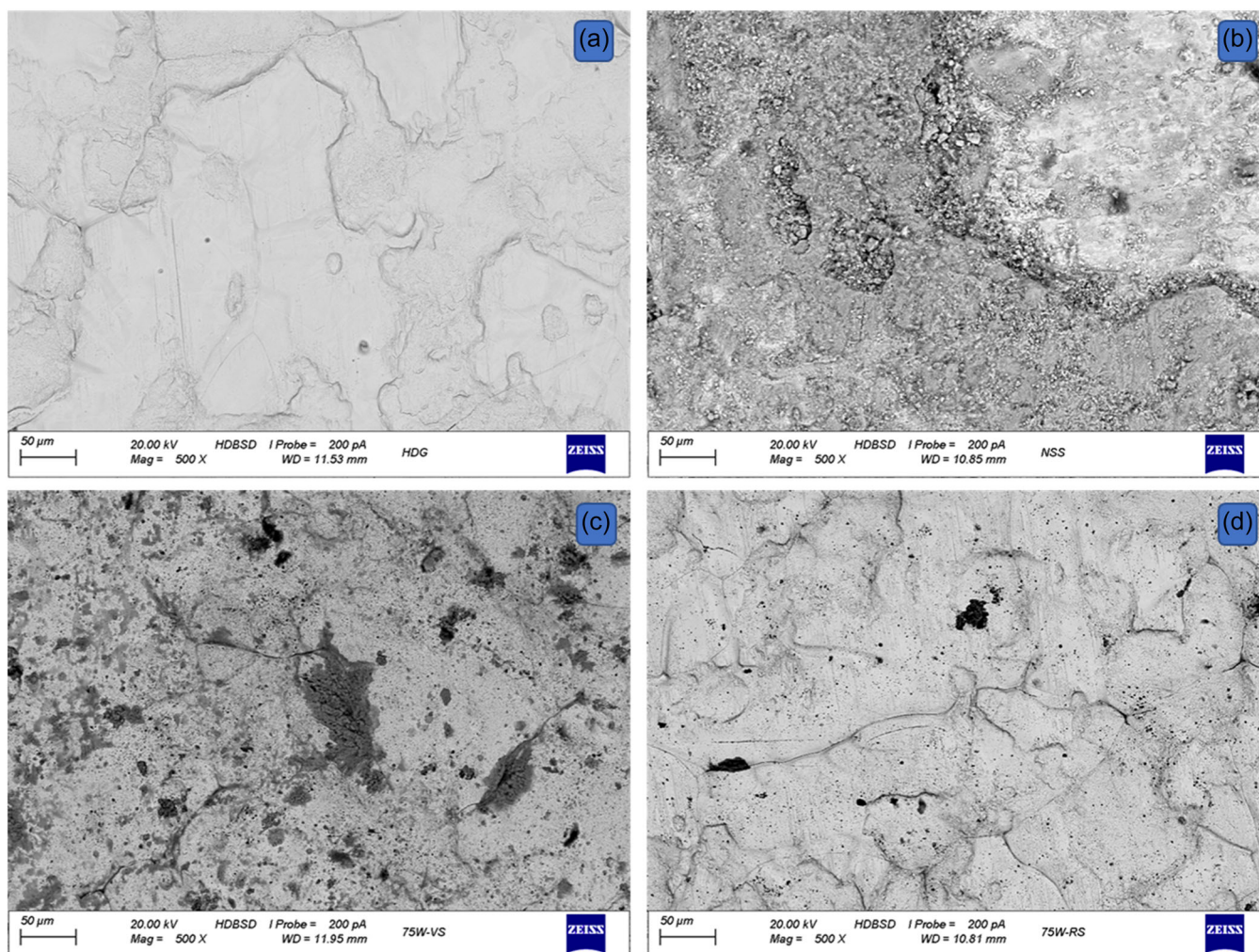


FIGURE 8 Comparative representation of the sample states: (a) HDG original, (b) HDG 7 days NSS, (c) HDG after 75 weeks exposure in C2 atmosphere top side, and (d) bottom side, at $\times 500$ magnification. [Color figure can be viewed at [wileyonlinelibrary.com](https://onlinelibrary.wiley.com/terms-and-conditions)]

TABLE 2 Results of the electrochemical investigations on the Lenne Bridge; individual measurements for each case.

| Measuring point | Potential after 5 min, mV | LPR after 10 min, $k\Omega\text{ cm}^2$ | Z' at 0.1 Hz, $k\Omega\text{ cm}^2$ | Z' at 10 kHz, $k\Omega\text{ cm}^2$ |
|------------------|---------------------------|---|---------------------------------------|---------------------------------------|
| Arch top side | -498 | 47 | 47 | 0.7 |
| Arch bottom side | -600 | 165 | 376 | 2.8 |
| Post with layer | -912 | 404 | 181 | 1.2 |
| Post activated | -925 | 12 | 11 | 0.6 |

varied exposure. This was determined through swipe samples and analysis of the contents of corrosive ion components. Figure 9 schematically shows the measurement points, with A and B being the external surfaces, C the bottom side, and D and E the internal surfaces. This is due to the sheltered exposure against the major air stream at the back side (E and D) of the girder. On the internal surfaces of the girder, pollutants can accumulate

as washing off by rainwater is unlikely. Elevated levels of sulfate ions (320.6 mg/m^2), chloride ions (32.8 mg/m^2), and nitrate ions (24.5 mg/m^2) were found there at the time of measurement. The ions were below the detection threshold on the external surfaces.

The values from the electrochemical measurements are compiled in Table 3. The protective layer resistances were determined three to five times each. The

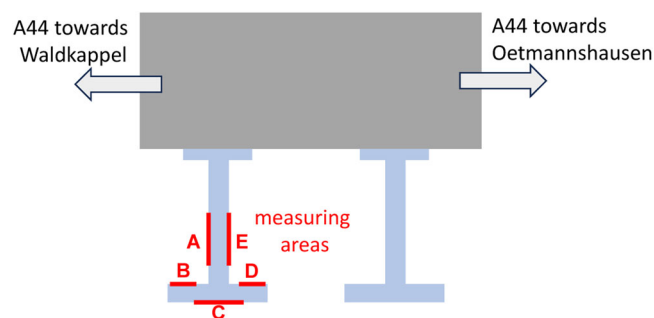


FIGURE 9 Measurement points A to E on a girder of the Waldkappel Motorway Bridge. [Color figure can be viewed at wileyonlinelibrary.com]

TABLE 3 Results of the electrochemical investigations on the Waldkappel Motorway Bridge; individual measurements for each case.

| Measurement point | Potential after 5 min, mV | LPR after 10 min, $k\Omega\text{ cm}^2$ | Z' at 0.1 Hz, $k\Omega\text{ cm}^2$ | Z' at 10 kHz, $k\Omega\text{ cm}^2$ |
|-------------------|---------------------------|---|---------------------------------------|---------------------------------------|
| A | -852 | 121 | 76 | 0.2 |
| B | -851 | 176 | 29 | 0.6 |
| C | -627 | 332 | 119 | 0.2 |
| D | -929 | 6 | 0.3 | 0.2 |
| E | -843 | 43 | 6 | 0.1 |

potential values and impedances represent individual measurements.

At the external measurement points A and B, the potential values are nearly identical at about -850 mV . Measurement point C (the bottom side of the girder) shows a significantly more positive potential value. Here, the protective layer resistance is higher at $332\text{ k}\Omega\text{ cm}^2$ compared to the external measurement points A and B, which have lower average values of 121 and $176\text{ k}\Omega\text{ cm}^2$, respectively.

The internally located measurement points show varying potential values. At measurement point D, the potential is significantly more negative, but the protective layer resistance is very low at only $6\text{ k}\Omega\text{ cm}^2$. At measurement point E, the average protective layer resistance is comparatively low at $43\text{ k}\Omega\text{ cm}^2$, though the potential is in the range of the external measurement points A and B. The lower protective layer resistances on the internal surfaces correlate with the higher level of corrosive ions found on these surfaces. It can be assumed that these ions have led to the formation of less protective layers. This increases the probability of higher corrosion rates at these points if corrosive conditions are also present.

TABLE 4 Results of the swipe samples on the Motorway Guardrail near Bergisch Gladbach.

| | Zn (piece-galvanized guardrail) | ZnAl (continuous hot-dip galvanized guardrail) |
|--------------------|---------------------------------|--|
| Cl^- | 6.0 mg/m^2 | 4.1 mg/m^2 |
| NO_3^- | 8.0 mg/m^2 | 1.8 mg/m^2 |
| SO_4^{2-} | 8.5 mg/m^2 | 5.5 mg/m^2 |

3.2.3 | Measurements on object 3: “Motorway Guardrails in Bergisch Gladbach”

The measurement campaign on the guardrails involved two objects, a piece-galvanized and a continuous HDG guardrail with a zinc–aluminum coating (ZnAl). Analyses of the conducted swipe samples, presented in Table 4, showed that there is no high accumulation of corrosive components on the freely weathered surfaces, which would be expected due to the proximity to the motorway. Besides rainfall events, subsequent spray mist events also help wash off corrosive deposits. However, during the winter months with de-icing salt use, these will surely contribute to chloride loading.

The electrochemical results presented in Table 5, indicate an extremely high protective layer resistance, suggesting low corrosion activity due to the effective protection. The OCPs are nearly identical and can be attributed to the protective layer resistance of similar magnitude. Impedance values for 0.1 and 1000 Hz are also comparable.

4 | DISCUSSION

4.1 | Comparison of values determined at practical objects and galvanized steel sheets

Electrochemical parameters such as currents or resistances provide valuable information that can effectively describe the current state of corrosion protection systems. The use of gel electrolytes for electrochemical measurements on exposed samples and practical objects has proven to be feasible.

The measurement results on samples of galvanized steel in their original and pickled states, after 7 days of exposure in a standard salt spray test, and after varying periods of time on a weathering test stand, demonstrate that simple electrochemical parameters can effectively differentiate between protective layers of varying degrees and compositions. The range of LPR values for samples

TABLE 5 Results of the electrochemical investigations on the Bergisch Gladbach Motorway Guardrail; individual measurements for each case.

| Measuring point | Potential after 5 min, mV | LPR after 10 min, $k\Omega\text{ cm}^2$ | Z' at 0.1 Hz, $k\Omega\text{ cm}^2$ | Z' at 10 kHz, $k\Omega\text{ cm}^2$ |
|--|---------------------------|---|---------------------------------------|---------------------------------------|
| Zn (piece-galvanized guardrail) | −811 | 720 | 113 | 1.2 |
| ZnAl (continuous hot-dip galvanized guardrail) | −835 | 640 | 136 | 0.9 |

after the NSS is in the lower $k\Omega\text{ cm}^2$ range, lower than those for a sample with surfaces in the delivery state or pickled surfaces, which exhibit values in the tens of $k\Omega\text{ cm}^2$ range. In contrast, weathered samples show LPR values in the mid-three-digit $k\Omega\text{ cm}^2$ range, where apparent differences due to microclimates exist (top side rained upon, bottom side ventilated and not rained upon).

LPR values of similar magnitudes were also measured on practical objects with several years of weathering history. The low LPR values could be associated with either a changed microclimate or the deposition of corrosive ions (girder of the Waldkappel Motorway Bridge). For the Lenne Bridge practical object, there was apparently already partial degradation of the iron–zinc alloy layer, visually identifiable by a brownish surface coloration. This is likely the reason for values only in the mid-two-digit $k\Omega\text{ cm}^2$ range. This condition of partial loss of the zinc coating can occur in hot-dip galvanizing after decades of use. All other values mostly fall within ranges measured on model samples under normal weathering after at least 1 year.

The results of the investigations presented here demonstrate a promising measurement approach, using gel electrolytes and portable electrochemical measurement technology, to obtain conclusive and practically relevant parameters for the current state of galvanized steel under atmospheric weathering. Subsequently, the potential applicability of the measurement results is presented and discussed.

4.2 | Considerations on the practical use of the electrochemical parameter R_L from LPR measurements for estimating current and future corrosion rates

As shown by the measurements on model samples with different corrosion histories and practical objects, there are significant differences in the determined protective layer resistances (R_L) determined by LPR measurements. These differences are primarily due to the types of protective layers that have formed over the course of various exposures, which determine the electrochemical

reactions under the chosen test conditions. For protective layers on zinc, it is mainly the cathodic partial reaction (oxygen reduction) that influences the protective layer resistance and thus the corrosion current density or the current corrosion rate. The nature and composition of the protective layer, as well as its bound components, are part of the corrosion history and significantly determine the subsequent corrosion behavior, provided the exposure conditions otherwise remain largely constant. The ability to characterize these protective layers minimally invasively using low-corrosivity gel electrolytes has been demonstrated here. Of practical relevance is now the question of whether and how these values can be used to estimate the current and future corrosion rate. The following additional factors must be considered for this purpose.

First, it must be assumed that the protective layer formation has entered a phase where it has completed on the majority of the surface and stabilized, that is, it does not significantly chemically transform further due to fluctuations in exposure (strong differences in wetting and access of pollutants). It is also presupposed that the coating degradation has not advanced to the extent that partially exposed steel substrate causes an inhomogeneous protective layer. Therefore, a stabilization phase is assumed, where the protective layer resistances only change slightly upwards or downwards.

Furthermore, an understanding of the actual time of wetness of the surface is needed to estimate the portion of time during which corrosion reactions are possible. This appears to be the most challenging part of the considerations, as the wetting duration, as defined for example in ISO 9223^[1] (time with $T > 0^\circ\text{C}$ and relative humidity $> 80\%$), fails in practice due to many conditions and influencing factors, such as the mass of the component or surface contaminations with substances that alter the saturation humidity and thus the effective wetting duration. On the other hand, it is precisely this factor (wetting conditions) that can lead to the formation of differently stable protective layers. Therefore, this influence is at least partially included in the protective layer resistance. The composition and protective effect of the layer can be seen as a kind of

“fingerprint” of previous exposure conditions. The dependence on rain events or moisture conditions was shown in Babutzka^[27]; they are necessary for protective layer formation.

Assuming these conditions, it is relatively easy to estimate the corrosion current density i_{corr} and future corrosion rate, as the following example calculations show. However, the conversion of the R_L to i_{corr} based on the Stern–Geary relationship^[28] requires the consideration of further electrochemical parameters. With the aid of the Tafel slopes in the anodic and cathodic areas of a polarization curve (b_a and b_c), the so-called B value can be calculated, by which the LPR is divided. The following formula according to Stern and Geary^[28] summarizes this.

$$i_{\text{corr}} = \frac{B}{R_L} = \frac{1}{R_L} \cdot \frac{b_a \cdot b_c}{2.303 \cdot (b_a + b_c)}. \quad (1)$$

The B value can be determined through preliminary experiments under identical conditions or by referencing literature values, such as those suggested by Metikos-Hutkovicz for galvanized steel under atmospheric conditions, proposing a B value of 13.8 mV/dec.^[29] Babutzka and Heyn established a relationship between the B value and the LPR value for zinc that has been weathered for varying lengths of time, demonstrating that the B value decreases as the LPR value increases.^[30] This relationship could be used for a dynamic B value correction, as there is a wide range of R_L values for protective layers on zinc surfaces. For simplicity, a constant B value, such as 15 mV/dec, can also be used. Since the B value decreases with higher R_L values (more stable protective layers), this would result in slightly overestimating the material loss, which, however, is a conservative approach concerning expected corrosion rates. Table 6 shows model calculations for various measurement points on practical objects and states after a 7-day salt spray test (reference for severe corrosion) and 75 weeks of exposure in a C2 atmosphere. A TOW value of 38% (equivalent to 3329 h/year), derived from research findings,^[24] was assumed. The Waldkappel Bridge example illustrates that significant differences in corrosivity can be induced on a component solely based on varying environmental impacts.

As expected, the predicted corrosion rate for the 7-day NSS sample is highest, exceeding 100 $\mu\text{m/a}$. The underlying R_L value here refers to the dried and cleaned sample surface after the test. Directly in the salt spray test, the value would likely be even lower, as it is evident that within 7 days, the 20 μm zinc coating was partially dissolved down to the steel. Theoretically, this suggests a corrosion rate in the salt spray test of >1000 $\mu\text{m/a}$, thus far from values under atmospheric exposure.

The 75-week weathered sample in a C2 atmosphere has a predicted corrosion rate of 0.3 $\mu\text{m/a}$, which falls precisely within the expected range for this exposure, as per ISO 9223,^[1] which is between 0.1 and 0.7 $\mu\text{m/a}$ (after the first year of exposure); see also Table 6. This range also includes the majority of the measurement points on practical objects. The range spans from 0.1 $\mu\text{m/year}$ (motorway guardrails) to about 0.7 $\mu\text{m/a}$ (outside of galvanized steel girders, Waldkappel Motorway Bridge). Notably, certain areas with detected contaminations of corrosive substances (inside of galvanized steel girders, Waldkappel Motorway Bridge) show significantly lower LPR values, resulting in predicted corrosion rates between 2 and 14 $\mu\text{m/a}$. Similarly, a galvanized steel beam at the Lenne Bridge, with a slightly higher rate of just over 2 $\mu\text{m/a}$, is notable. This can be explained by the visually apparent degradation of the zinc coating, indicating increased corrosion.

The conversion of the determined corrosion rate into corrosivity categories is not standardized due to the age of the samples. However, the description of the coating kinetics through LPR, derivation of the R_L , and determination of the corrosion rate based on a fixed B value reflects the protective effect that a formed protective layer can have, depending on the corrosivity of the respective atmosphere. This can ultimately be reflected in a representation in C categories to be able to estimate the prevailing corrosivity and ultimately also the service life of a structure depending on the zinc coating thickness.

5 | SUMMARY AND CONCLUSIONS

Determining the corrosion rate of galvanized steel under atmospheric exposure is challenging due to typically very low material loss rates of well below 1 $\mu\text{m/a}$. Direct measurements of zinc coating thickness or mass loss on components are nearly impossible. Therefore, the use of electrochemical methods to determine corrosion current densities or protective layer resistances on exposed samples or real structures is a promising approach.

Since an electrolyte is required for the electrochemical determination of a parameter that can describe the protective effect of a layer under atmospheric conditions, it must be selected to closely resemble or adequately reflect these conditions. Liquid electrolytes, which do not correspond to the conditions of a thin electrolyte film, are not suitable. Furthermore, liquid electrolytes are more cumbersome to handle. In contrast, the use of gel electrolytes is based on the application of agar-based gels with very low contents of corrosive ions as an

TABLE 6 Corrosion rate forecast for model samples and measurement points on practical objects using averaged R_L values for each measurement point or exposure condition, a constant assumed B value of 15 mV/dec, and an average TOW of 38% (except for NSS).

| Measuring point | Mean R_L -value (k Ω cm ²) | Feature | Assumed TOW | Forecast corrosion rate | C-class according to 9223 |
|---|---|-----------------------|---------------|-------------------------|---------------------------|
| <i>Model samples</i> | | | | | |
| HDG 7 days NSS | 2.1 | 100% Wet + salt | 100%/8760 h/a | 104.7 μ m/a | >CX |
| HDG 75 W top side | 330 | Without contamination | 38%/3329 h/a | 0.3 μ m/a | C2 |
| <i>Practical object: Lenne Bridge</i> | | | | | |
| Arch top side | 47 | Without contamination | 38%/3329 h/a | 2.0 μ m/a | C3 |
| Arch bottom side | 165 | Without contamination | 38%/3329 h/a | 0.5 μ m/a | C2 |
| Post with layer | 404 | Without contamination | 38%/3329 h/a | 0.3 μ m/a | C2 |
| <i>Practical object: Waldkappel Motorway Bridge</i> | | | | | |
| A (outside) | 121 | Without contamination | 38%/3329 h/a | 0.7 μ m/a | C2 (C3) |
| B (outside) | 176 | Without contamination | 38%/3329 h/a | 0.5 μ m/a | C2 |
| C (bottom) | 322 | Without contamination | 38%/3329 h/a | 0.3 μ m/a | C2 |
| D (inside) | 6 | With contamination | 38%/3329 h/a | 14.2 μ m/a | CX |
| E (inside) | 43 | With contamination | 38%/3329 h/a | 2.0 μ m/a | C3 |
| <i>Practical object: Motroway Guardrails in Bergisch Gladbach</i> | | | | | |
| Guardrail piece-galvanized Zn | 720 | Slight contamination | 38%/3329 h/a | 0.1 μ m/a | C2 |
| Guardrail continuous hot-dip galvanized ZnAl | 640 | Slight contamination | 35%/3329 h/a | 0.1 μ m/a | C2 |

electrolyte, allowing potentially present corrosive species from the protective layers to dissolve in the forming electrolyte film between the gel and the metal surface, thus simulating the wetting of the surface as it would occur in practice. After an application time of 10 min, acceptable steady states are reached, and subsequent electrochemical measurements can be performed. The handling is considerably simpler and can be implemented on-site.

The results shown here on model samples subjected to various corrosion conditions demonstrate that zinc samples without a protective layer, samples under strong artificial corrosive exposure (NSS), and atmospheric exposure can be distinctly differentiated using LPR measurements with gel electrolytes to determine the layer resistance R_L . The use of these electrolytes opens the possibility of also measuring real structures and components, thereby demonstrating the influence of corrosion-determining factors. These could be, for example, the impact of local microclimates that determine the stability of protective layers and thus the future material loss or lifespan of zinc coatings. Measurements on three typical practical objects have shown that the measurements can be carried out relatively easily and lead to comprehensible results. A correlation of the measured values with typical exposure conditions, microclimates, or contaminations of the surfaces with corrosive species was observed.

A derivation of the current or future corrosion rate from the measured protective layer resistances can be made using an average expected time of wetness. With this simple approach, comprehensible values emerge, which one can expect for galvanized steel after exposure, often falling in the range below 1 $\mu\text{m}/\text{year}$. Furthermore, it was demonstrated that in areas with contaminations of corrosive anions, the protective layer resistances are lower, resulting in significantly higher predicted corrosion rates, which also meets expectations. At spots where defects in the coating have already occurred due to enhanced corrosion, lower resistance values are also measured, which, however, do not reflect the R_L of the zinc coating. Nevertheless, higher corrosion rates can also be expected in these areas if corrosive conditions are present.

In summary, it can be said that electrochemical measurements using gel electrolytes are suitable for obtaining valuable information about the current corrosion state of structures with galvanized steel. To enable these measurements to be reproducibly conducted by professionals, a standard^[31] has been drafted, detailing the procedure and will soon be available.

AUTHOR CONTRIBUTIONS

Andreas Heyn: Conceptualization; methodology; formal analysis; writing—original draft; visualization; project

administration; funding acquisition. **Moritz Meist:** Investigation. **Oliver Michael:** Investigation. **Martin Babutzka:** Investigation; project administration; funding acquisition; review and editing. **Svenja Valet:** Investigation; writing—review and editing; project administration. **Gino Ebell:** Review and editing.

ACKNOWLEDGMENTS

Dr. Heyn would like to thank the German Research Foundation (DFG) for funding the project “Agar-based gel-electrolytes for corrosion diagnostic” (project number 330472124). This work was supported by the Federal Ministry for Economic Affairs and Energy in the frame of the WIPANO project GELELEK FKZ 03TNH014A.

CONFLICT OF INTEREST STATEMENT

The authors declare no conflict of interest.

DATA AVAILABILITY STATEMENT

The data that support the findings of this study are available from the corresponding author upon reasonable request.

ORCID

Andreas Heyn  <https://orcid.org/0000-0002-0146-219X>

Oliver Michael  <https://orcid.org/0009-0001-9249-0443>

Martin Babutzka  <https://orcid.org/0000-0002-3074-2203>

Svenja Valet  <https://orcid.org/0000-0001-5158-2483>

Gino Ebell  <http://orcid.org/0000-0002-6006-2460>

REFERENCES

- [1] ISO 9223:2012, Corrosion of metals and alloys—Corrosivity of atmospheres—Classification, determination and estimation **2012**.
- [2] ISO 9226:2012, Corrosion of metals and alloys—Corrosivity of atmospheres—Determination of corrosion rate of standard specimens for the evaluation of corrosivity **2012**.
- [3] ISO 9224:2012, Corrosion of metals and alloys—Corrosivity of atmospheres—Guiding values for the corrosivity categories **2012**.
- [4] ISO 8565:2011, Metals and alloys—Atmospheric corrosion testing—General requirements **2011**.
- [5] M. Babutzka, A. Burkert, A. Heyn, *16. Sommerkurs Werkstoffe und Fügen*, Otto von Guericke University Library, Magdeburg, Germany **2017**, p. 119. <https://doi.org/10.25673/5172>
- [6] I. Odnevall, C. Leygraf, *Corros. Sci.* **1993**, *34*, 1213.
- [7] I. Odnevall, C. Leygraf, *Corros. Sci.* **1994**, *36*, 1551.
- [8] I. Odnevall, C. Leygraf, *Corros. Sci.* **1994**, *36*, 1077.
- [9] D. Persson, D. Thierry, O. Karlsson, *Corros. Sci.* **2017**, *126*, 152.
- [10] I. Odnevall Wallinder, C. Leygraf, *Corrosion* **2017**, *73*, 1060.
- [11] G. Ji, K. Baert, B. Allaert, A. Hubin, H. Terryn, *Corros. Eng., Sci Technol.* **2020**, *55*, 562.

- [12] J. W. Fulton, D. F. Swinehart, *J. Am. Chem. Soc.* **1954**, *76*, 864.
- [13] B. Mao, *PhD Thesis*, University of Bordeaux **2017**.
- [14] A. Heyn, *IOP Conf. Ser.: Mater. Sci. Eng.* **2020**, *882*, 012010.
- [15] E. Cano, A. Crespo, D. Lafuente, B. Ramirez Barat, *Electrochem. Commun.* **2014**, *41*, 16.
- [16] G. Monrrabal, B. Ramírez-Barat, A. Bautista, F. Velasco, E. Cano, *Metals* **2018**, *8*, 500.
- [17] G. Monrrabal, A. Bautista, F. Velasco, *Corrosion* **2019**, *75*, 1502.
- [18] J. Vanbrabant, N. van de Velde, Proceedings European General Galvanizers Association Intergalva, Berlin **2000**, *19*, 29/1.
- [19] M. Babutzka, A. Heyn, *IOP Conf. Ser.: Mater. Sci. Eng.* **2016**, *118*, 17.
- [20] M. Babutzka, A. Heyn, *IOP Conf. Ser.: Mater. Sci. Eng.* **2017**, *181*, 012021.
- [21] A. Heyn, Forschungsseminar des MDZWP 2021, Magdeburg **2021**. <https://doi.org/10.13140/RG.2.2.36660.78721>
- [22] U. Langklotz, M. Babutzka, M. Schneider, A. Burkert, *Mater. Corros.* **2019**, *70*, 1314.
- [23] S. Valet, A. Burkert, G. Ebell, M. Babutzka, *Electrochim. Acta* **2021**, *385*, 138191.
- [24] A. Heyn, *16. Sommerkurs Werkstoffe und Fügen*, Magdeburg **2017**, p. 129. https://www.researchgate.net/publication/322100415_Korrosionsuntersuchungen_mit_gelartigen_Elektrolyten_zur_Beschreibung_der_Korrosionsschutzwirkung_von_Zinkuberzugen
- [25] DIN EN ISO 9227:2017-07, Corrosion tests in artificial atmospheres—Salt spray tests **2017**.
- [26] S. Valet, T. Bohlmann, A. Burkert, G. Ebell, *J. Electroanal. Chem.* **2023**, *948*, 117814.
- [27] M. Babutzka, *PhD Thesis*, RWTH Aachen University (Düren) **2020**.
- [28] M. Stern, A. L. Geaby, *J. Electrochem. Soc.* **1957**, *104*, 56.
- [29] M. Metikoš-Huković, C. Zevnik, *Mater. Corros.* **1984**, *35*, 116.
- [30] M. Babutzka, A. Heyn, *IOP Conf. Ser.: Mater. Sci. Eng.* **2017**, *181*, 012021. <https://iopscience.iop.org/article/10.1088/1757-899X/181/1/012021>
- [31] DIN EN ISO 50023, Draft, Corrosion of metals and alloys—Electrochemical test methods—Test method for the determination of surface resistivity of zinc and zinc coatings using gel electrolytes **2024**.

How to cite this article: A. Heyn, M. Meist, O. Michael, M. Babutzka, S. Valet, G. Ebell, *Mater. Corros.* **2024**, 1–16. <https://doi.org/10.1002/maco.202414389>